Supporting Information

Semi-Quantitative Assessment of Intersystem Crossing Rate: An Extension of El-Sayed Rule to the Emissive Transition Metal Complexes

Elise Yu-Tzu Li[1], Tzung-Ying Jiang[1], Yun Chi[2] and Pi-Tai Chou[3*]*

Affiliations:

[1] Department of Chemistry, National Taiwan Normal University, Taipei 106, Taiwan

[2] Department of Chemistry, National Tsing Hua University, Hsinchu 300, Taiwan

[3] Department of Chemistry and Center for Emerging Material and Advanced Devices, National Taiwan University, Taipei 106, Taiwan

*e-mail: eliseytli@ntnu.edu.tw; chop@ntu.edu.tw

Table S1. Calculated excitation energies, MLCT percentage and orbital transition analyses for lowest singlet excited states and selected higher excited states of **Os-1** to **Os-5** complexes that show strong MLCT characteristics computed by TDDFT/scalar relativistic ZORA/PCM (CH_2Cl_2) at optimized ground states geometries.

complex	state	Oscillator strength(f)	assignment	Excitation energy (ev)	MLCT(%)
Os-1	S_1	0.2546	H→L(99%)	2.33	0
	S_4	0.0051	H→L+2(99%)	3.59	-10
	T_1	0	H→L(80%)	1.69	0

	T_7	0	H→L+3(93%)	3.64	-8
	T_8	0	H→L+4(35%), H→L+6(29%), H- 1→L+1(13%)	3.78	-5
Os-2	S_1	0.3767	H→L(99%)	2.92	0
	S_3	0.0991	H-2→L(93%)	3.91	10
	T_1	0	H→L(83%)	2.38	0
	T_6	0	H→L+2(61%), H-3→L(8%) H-5→L(5%)	4.08	-3
	T_7	0	H→L+2(29%), H-3→L(17%) H-5→L(16%), H-4→L(10%)	4.09	7
	T_8	0	H→L+6(43%), H-4→L(25%) H-6→L(6%),	4.16	9
Os-3	S_1	0.6210	H→L(97%)	3.63	4
	T_1	0	H→L(90%), H-2→L(5%)	2.67	4
	T_4	0	H-4→L(58%), H-5→L(22%) H-7→L(8%), H-3→L(7%)	4.17	26
	T_5	0	H→L+1(38%), H-3→L(20%)	4.25	4
	T_6	0	H-3→L(44%), H-1→L(5%)	4.28	16
Os-4	S_1	0.0772	H→L(92%), H-4→L(5%)	3.86	16

	T_1	0	H→L(92%), H-4→L(5%)	2.58	17
	T_2	0	H-1→L(96%)	3.97	39
	T_3	0	H-2→L(53%), H-3→L(42%)	4.05	27
	T_4	0	H-5→L(83%), H-6→L(13%)	4.37	19
Os-5	S_1	0.0354	H→L(99%)	3.05	61
	T_1	0	H→L(92%)	2.84	57
	T_2	0	H-1→L(61%), H-3→L(14%)	3.26	8
	T_4	0	H→L+1(65%), H→L+2(12%) H-1→L(5%)	3.48	48
	T_5	0	H-3→L(52%) ,H-4→L(16%)	3.74	15
	T_8	0	H-2→L(92%)	3.83	65

Table S2. Calculated excitation energies, MLCT percentage and orbital transition analyses for lowest singlet excited states and selected higher excited states of **Cu-1** and **Cu-2** complexes that show strong MLCT characteristics computed by TDDFT/scalar relativistic ZORA/PCM (CH_2Cl_2) at optimized ground states geometries.

Excitation state	Oscillator strength(f)	assignment	Excitation energy	MLCT(%)
Cu-1				
S_1	0.1409	H→L(98%)	3.21	40
T_1	0	H→L(92%)	3.02	38
T_2	0	H-2→L(83%)	3.11	1

T_3	0	H-1→L(91%)	3.25	60
T_9	0	H-3→L(83%)	3.66	50
T_{10}	0	H→L+6(26%), H→L+7(12%) H→L+4(8%), H-3→L(7%)	3.69	25
Cu-2				
S_1	0.0826	H→L(96%)	2.67	45
T_1	0	H→L(90%)	2.47	42
T_2	0	H-2→L(71%), H-1→L(11%) H-7→L(6%)	2.63	13
T_3	0	H-1→L(83%), H-2→L(10%)	2.81	59
T_4	0	H-3→L(44%), H-7→L(25%) H-4→L(8%), H-6→L(6%)	3.09	36
T_5	0	H-3→L(52%), H-7→L(20%) H-4→L(9%), H-2→L(8%)	3.10	38
T_9	0	H-4→L(30%), H-5→L(28%) H-7→L(23%)	3.53	35

Table S3. Calculated excitation energies, MLCT percentage and orbital transition analyses for lowest singlet excited states and selected higher excited states of **Ag-1** and **Ag-2** complexes that show strong MLCT characteristics computed by TDDFT/scalar relativistic ZORA/PCM (CH_2Cl_2) at optimized ground states geometries.

Excitation state	Oscillator strength(f)	assignment	Excitation energy	MLCT(%)
Ag-1				
S_1	0.0669	H→L(98%)	3.71	21
T_1	0	H-1→L(53%), H-1→L+1(26%)	3.23	0
T_2	0	H→L+2(56%)	3.50	14
T_3	0	H→L(47%), H→L+1(26%)	3.54	15
T_4	0	H→L+1(22%), H→L(19%) H→L+3(13%), H→L+2(9%)	3.64	14
T_{11}	0	H-2→L+6(31%), H-2→L+1(19%) H-3→L(16%), H-4→L(6%)	3.91	15
Ag-2				
S_1	0.1245	H→L(96%)	3.25	19
T_1	0	H-1→L(76%), H-5→L(12%)	2.69	0.5
T_2	0	H-5→L(46%), H→L(34%) H-2→L(6%)	3.10	9
T_3	0	H→L(58%), H-5→L(16%) H-1→L(12%), H-4→L(8%)	3.21	14

T_4	0	H-3→L(16%), H→L+2(16%) H-2→L(15%), H-4→L(14%)	3.52	12
T_5	0	H→L+2(16%), H-3→L(14%) H-2→L(13%), H-4→L(12%)	3.53	10

Table S4. Calculated excitation energies, MLCT percentage and orbital transition analyses for lowest singlet excited states and selected higher excited states of **Au-1** and **Au-2** complexes that show strong MLCT characteristics computed by TDDFT/scalar relativistic ZORA/PCM (CH_2Cl_2) at optimized ground states geometries.

Excitation state	Oscillator strength(f)	assignment	Excitation energy	MLCT(%)
Au-1				
S_1	0.4736	H→L(83%), H→L+2(10%)	3.94	0
S_2	0.0548	H-1→L(83%), H-1→L+2(17%)	4.21	17
T_1	0	H→L(62%), H→L+2(21%)	3.17	0
T_2	0	H-3→L+2(18%), H-1→L(15%)	3.80	4
T_3	0	H-1→L+1(17%), H-3→L+1(15%) H-8→L+2(5%)	3.81	4
T_4	0	H-7→L+1(11%), H-3→L+3(10%) H-8→L+2(7%), H-8→L(7%)	3.84	2
T_5	0	H-1→L(39%), H-1→L+2(20%), H-3→L(11%)	3.88	13
T_7	0	H→L+1(26%), H-2→L(21%) H→L(12%), H→L+2(11%), H-2→L+2(7%)	4.17	2
T_8	0	H→L+1(27%), H-2→L(36%) H→L(9%), H→L+2(6%) , H-2→L+2(10%)	4.23	4
Au-2				
S_1	0.5509	H→L(96%)	3.51	0

S_2	0.0286	H-2→L(48%), H-1→L(37%) ,H-4→L(11%)	3.88	9
T_1	0	H→L(67%), H-1→L(16%) ,H-2→L(11%)	2.76	2
T_2	0	H-1→L(49%), H→L(25%) ,H-2→L(14%)	3.21	5
T_3	0	H-2→L(55%), H-1→L(17%) ,H-4→L(16%)	3.58	9
T_8	0	H-4→L(71%)	4.00	7

Table S5. SOC integrals (in cm^{-1}) between S_n (n=1-10) and T_m (m=1-10) states of **Os-6** complex. The excited states are computed by TDDFT/scalar relativistic ZORA/PCM (CH_2Cl_2) at optimized ground states geometries. The maximal SOC integral is marked in red.

T_m (eV) / S_n (eV)		1	2	3	4	5	6	7	8	9	10
		2.39	3.17	3.56	3.69	3.87	3.94	3.98	4.13	4.27	4.38
1	3.15	0	50	19	30	92	0	37	7	19	83
2	3.82	56	14	0	175	89	0	104	16	131	76
3	4.02	0	0	0	0	0	0	0	60	21	0
4	4.10	17	158	65	82	275	0	99	25	96	246
5	4.13	35	96	38	124	148	25	35	20	110	127
6	4.24	0	72	40	14	131	54	53	10	27	119
7	4.29	67	102	35	124	193	22	93	22	114	170
8	4.38	0	97	33	112	157	0	54	16	95	141
9	4.49	84	49	11	**267**	160	0	169	26	201	139
10	4.61	21	50	17	58	94	0	64	0	33	98

Table S6. SOC integrals (in cm^{-1}) between S_n (n=1-10) and T_m (m=1-10) states of **Os-7** complex. The excited states are computed by TDDFT/scalar relativistic ZORA/PCM (CH_2Cl_2) at optimized ground states geometries. The maximal SOC integral is marked in red.

S_n (eV) \ T_m (eV)		1	2	3	4	5	6	7	8	9	10
		2.38	3.17	3.55	3.73	3.86	3.94	4.00	4.10	4.14	4.22
1	3.14	0	50	19	0	101	0	13	60	48	37
2	3.84	56	57	0	157	59	0	15	72	97	98
3	4.01	0	0	0	0	0	0	0	0	0	0
4	4.06	8	179	65	68	**294**	0	29	157	161	150
5	4.14	9	124	44	76	65	0	0	84	106	111
6	4.18	8	132	40	75	191	0	16	95	114	116
7	4.20	0	88	46	0	180	0	23	107	86	66
8	4.29	24	31	3	67	14	50	9	25	36	36
9	4.41	97	126	11	270	57	12	36	31	145	147
10	4.59	0	7	20	0	0	12	0	0	0	0

Table S7. SOC integrals (in cm^{-1}) between S_n (n=1-10) and T_m (m=1-10) states of **Os-8** complex. The excited states are computed by TDDFT/scalar relativistic ZORA/PCM (CH_2Cl_2) at optimized ground states geometries. The maximal SOC integral is marked in red.

T_m (eV) / S_n (eV)		1	2	3	4	5	6	7	8	9	10
		2.44	3.34	3.45	3.61	3.84	4.08	4.27	4.41	4.45	4.47
1	3.27	0	0	0	0	0	0	0	0	0	0
2	3.83	0	0	0	0	309	0	0	266	64	64
3	4.06	0	0	0	0	0	0	0	0	0	0
4	4.15	0	26	0	48	0	0	47	0	0	0
5	4.24	0	8	180	30	29	34	32	85	82	82
6	4.35	0	9	0	41	0	61	45	0	0	0
7	4.50	0	10	264	19	79	0	19	109	120	29
8	4.59	0	0	0	0	0	0	17	0	0	24
9	4.77	0	0	**374**	0	329	0	0	288	121	99
10	4.80	0	4	250	8	112	0	8	87	113	25

Table S8. SOC integrals (in cm^{-1}) between S_n (n=1-10) and T_m (m=1-10) states of **Os-9** complex. The excited states are computed by TDDFT/scalar relativistic ZORA/PCM (CH_2Cl_2) at optimized ground states geometries. The maximal SOC integral is marked in red.

T_m (eV) / S_n (eV)		1	2	3	4	5	6	7	8	9	10
		2.46	3.37	3.42	3.62	3.83	4.07	4.17	4.18	4.39	4.46
1	3.3	0	28	48	10	69	57	35	50	0	0
2	3.8	49	105	0	29	143	191	51	66	0	0
3	4.0	46	78	159	30	212	159	115	164	0	0
4	4.1	32	36	118	9	132	101	66	98	0	0
5	4.2	54	116	64	37	188	**208**	86	110	0	15
6	4.3	0	0	0	0	0	0	0	0	0	39
7	4.3	39	64	55	14	119	139	45	63	0	14
8	4.5	10	15	30	0	33	31	14	20	0	5
9	4.6	0	18	0	35	0	0	8	26	0	20
10	4.7	31	27	90	0	101	94	43	63	0	6

Table S9. The coefficients of osmium d orbitals in selected orbitals of **Os-1** to **Os-5** at optimized ground states geometries.

mo	d_{xy}	d_{xz}	d_{yz}	$d_{x^2-y^2}$	d_{z^2}
			Os-1		
H-5	0.43	0.16	0.17	0.29	0.11
H-4	0.19	0.55	0.16	0.13	0.15
H-3	0.00	0.12	0.00	0.00	0.00
H-2	0.11	0.10	0.16	0.14	0.14
H-1	0	0	0	0	0
H	0.00	0.00	0.00	0.00	0.00
L	0.00	0.00	0.00	0.00	0.00
L+2	0.11	0.18	0.13	0.19	0.00
L+3	0.00	0.00	0.17	0.00	0.24
L+4	0.10	0.15	0.21	0.00	0.14
L+6	0.00	0.15	0.13	0.00	0.12
			Os-2		
H-6	0.33	0.23	0.15	0.23	0.00
H-5	0.00	0.00	0.00	0.00	0.22
H-4	0.24	0.37	0.16	0.29	0.00
H-3	0.00	0.32	0.17	0.38	0.33
H-2	0.23	0.10	0.00	0.00	0.21
H	0.00	0.00	0.00	0.00	0.00
			Os-3		
H-5	0.00	0.00	0.00	0.21	0.00
H-4	0.33	0.18	0.00	0.19	0.00
H-3	0.32	0.20	0.00	0.37	0.22
H-2	0.16	0.38	0.32	0.17	0.25
H-1	0.20	0.24	0.00	0.14	0.11

H	0.13	0.00	0.00	0.00	0.15
Os-4					
H-6	0.00	0.14	0.41	0.00	0.00
H-5	0.00	0.21	0.18	0.00	0.00
H-4	0.36	0.00	0.00	0.59	0.00
H-3	0.25	0.00	0.00	0.11	0.57
H-2	0.23	0.00	0.00	0.13	0.34
H-1	0.00	0.31	0.56	0.00	0.00
H	0.17	0.00	0.00	0.33	0.10
Os-5					
H-5	0.00	0.00	0.10	0.00	0.00
H-4	0.16	0.17	0.49	0.16	0.34
H-3	0.00	0.00	0.22	0.14	0.11
H-2	0.19	0.77	0.24	0.11	0.00
H-1	0.13	0.00	0.27	0.00	0.15
H	0.59	0.23	0.00	0.46	0.00

Table S10. The c coefficients of copper d orbitals in selected orbitals of **Cu-1** and **Cu-2** at optimized ground states geometries.

mo	d_{xy}	d_{xz}	d_{yz}	$d_{x^2-y^2}$	d_{z^2}
Cu-1					
H-3	0.13	0.30	0.10	0.67	0.11
H-2	0.00	0.12	0.00	0.00	0.00
H-1	0.22	0.31	0.36	0.15	0.60
H	0.38	0.30	0.23	0.29	0.18
Cu-2					
H-7	0.00	0.00	0.00	0.00	0.33
H-6	0.38	0.11	0.22	0.14	0.53

H-5	0.57	0.13	0.28	0.56	0.00
H-4	0.00	0.25	0.22	0.00	0.55
H-3	0.31	0.42	0.52	0.00	0.26
H-2	0.00	0.13	0.00	0.00	0.21
H-1	0.23	0.65	0.44	0.14	0.11
H	0.37	0.00	0.20	0.54	0.00

Table S11. The c coefficients of silver d orbitals in selected orbitals of **Ag-1** and **Ag-2** at optimized ground states geometries.

mo	d_{xy}	d_{xz}	d_{yz}	$d_{x^2-y^2}$	d_{z^2}
			Ag-1		
H-4	0.00	0.11	0.13	0.36	0.18
H-3	0.11	0.00	0.13	0.17	0.33
H-2	0.00	0.23	0.25	0.00	0.28
H	0.30	0.17	0.15	0.20	0.17
			Ag-2		
H-5	0.00	0.17	0.00	0.00	0.10
H-4	0.00	0.49	0.00	0.12	0.14
H-3	0.21	0.16	0.27	0.00	0.00
H-2	0.23	0.00	0.18	0.00	0.12
H	0.17	0.00	0.18	0.37	0.00

Table S12. The c coefficients of gold d orbitals in selected orbitals of **Au-1** and **Au-2** at optimized ground states geometries.

mo	d_{xy}	d_{xz}	d_{yz}	$d_{x^2-y^2}$	d_{z^2}
			Au-1		
H-8	0.00	0.00	0.00	0.10	0.00
H-3	0.19	0.00	0.00	0.11	0.00

H-2	0.00	0.29	0.00	0.00	0.00
H-1	0.23	0.00	0.00	0.40	0.00
H	0.00	0.00	0.00	0.00	0.00
Au-2					
H-4	0.22	0.00	0.00	0.11	0.00
H-3	0.00	0.28	0.11	0.00	0.00
H-2	0.20	0.00	0.00	0.28	0.00
H-1	0.17	0.00	0.00	0.20	0.00
H	0.00	0.00	0.00	0.00	0.00

Table S13. The c coefficients of osmium d orbitals in selected orbitals of **Os-6** to **Os-9** at optimized ground states geometries.

mo	d_{xy}	d_{xz}	d_{yz}	$d_{x^2-y^2}$	d_{z^2}
Os-6					
H-6	0.00	0.11	0.22	0.00	0.00
H-5	0.00	0.38	0.21	0.00	0.00
H-4	0.00	0.00	0.10	0.00	0.00
H-3	0.00	0.00	0.00	0.22	0.00
H-2	0.00	0.00	0.44	0.00	0.00
H-1	0.00	0.24	0.15	0.00	0.00
H	0.00	0.00	0.14	0.00	0.00
L	0.00	0.00	0.00	0.00	0.00
L+1	0.24	0.00	0.13	0.00	0.12
L+3	0.00	0.00	0.00	0.00	0.19
Os-7					
H-5	0.00	0.46	0.16	0.00	0.00
H-4	0.00	0.00	0.00	0.00	0.00
H-3	0.00	0.00	0.47	0.00	0.00

H-2	0.00	0.11	0.00	0.17	0.00
H-1	0.00	0.25	0.13	0.00	0.00
H	0.00	0.00	0.14	0.00	0.00
Os-8					
H-8	0.00	0.53	0.15	0.19	0.24
H-7	0.21	0.13	0.24	0.69	0.00
H-5	0.00	0.00	0.35	0.00	0.14
H-4	0.12	0.20	0.00	0.24	0.00
H-3	0.00	0.20	0.38	0.21	0.00
H-1	0.00	0.27	0.22	0.00	0.19
H	0.00	0.00	0.00	0.00	0.00
L	0.00	0.00	0.00	0.00	0.00
L+1	0.21	0.00	0.00	0.00	0.19
L+2	0.00	0.00	0.12	0.00	0.00
L+3	0.00	0.00	0.00	0.00	0.15
Os-9					
H-6	0.00	0.22	0.00	0.00	0.00
H-5	0.00	0.29	0.37	0.00	0.00
H-4	0.00	0.14	0.00	0.00	0.00
H-3	0.00	0.00	0.23	0.16	0.00
H-2	0.00	0.28	0.32	0.00	0.00
H-1	0.00	0.00	0.11	0.00	0.00
H	0.00	0.00	0.00	0.00	0.00

Figure S1. Spatial plots (isovalue = 0.03) of selected molecular orbitals for **Os-1** at ground-state optimized geometry.

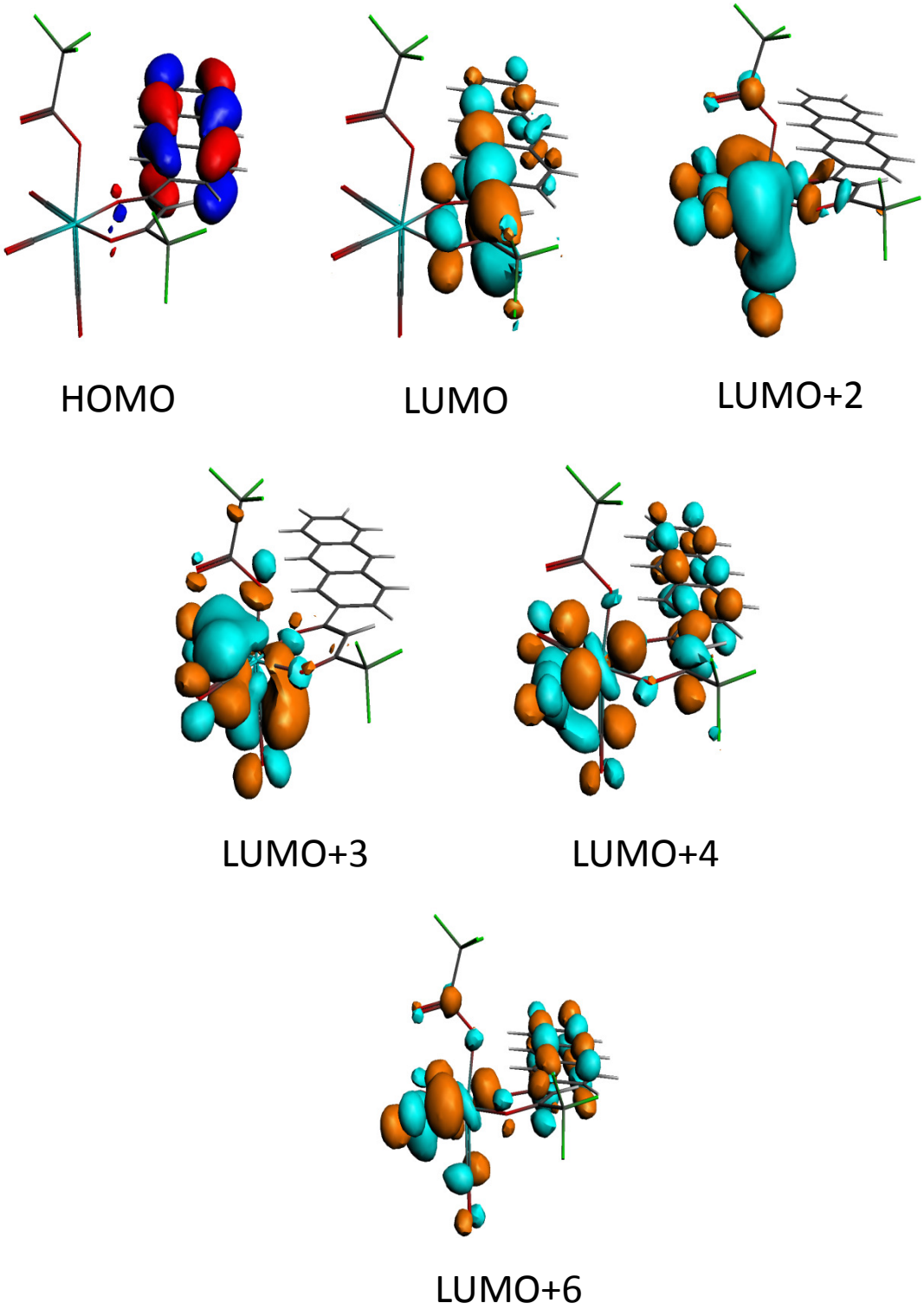

Figure S2. Spatial plots (isovalue = 0.03) of selected molecular orbitals for **Os-2** at ground-state optimized geometry.

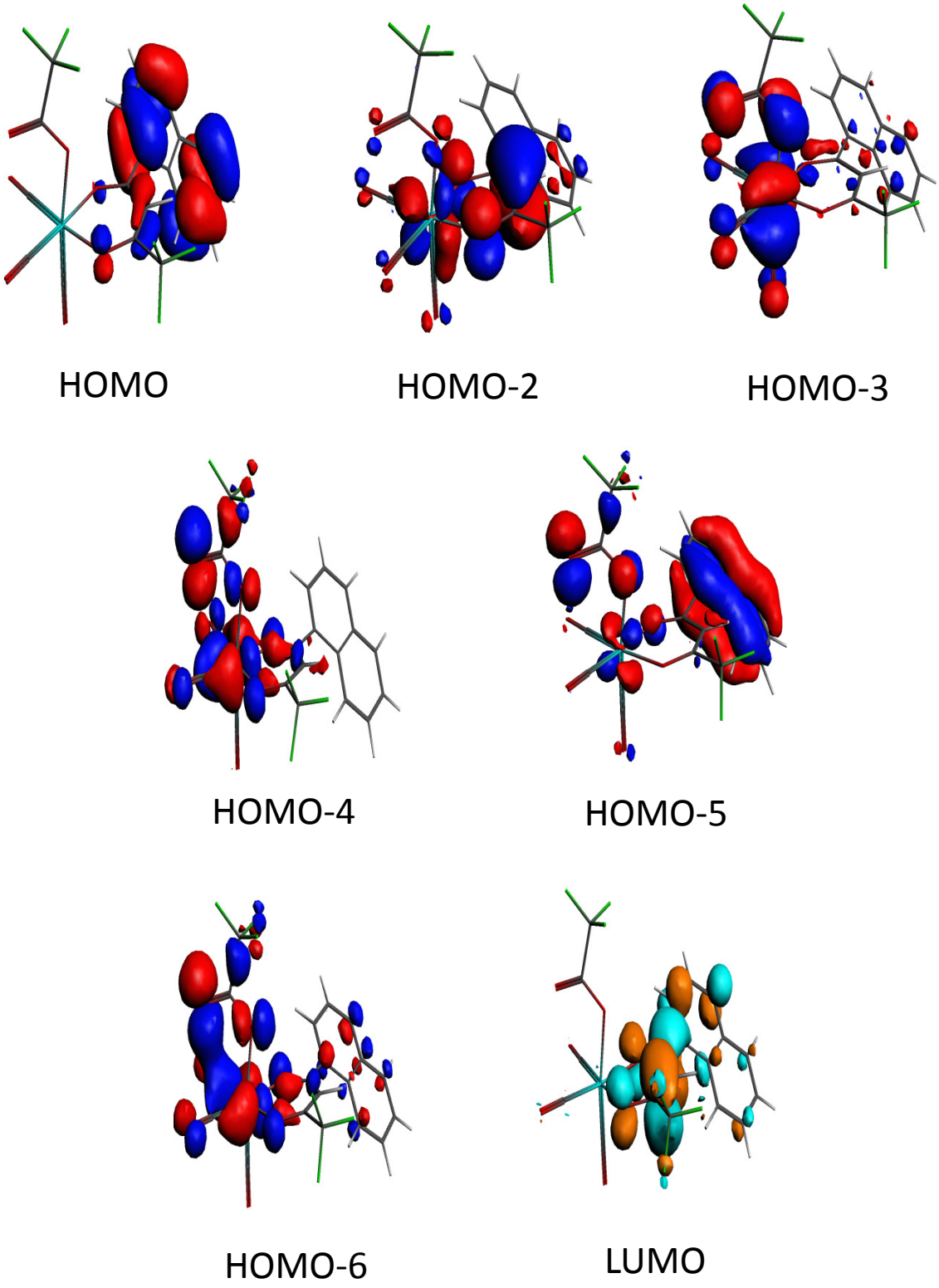

Figure S3. Spatial plots (isovalue = 0.03) of selected molecular orbitals for **Os-3** at ground-state optimized geometry.

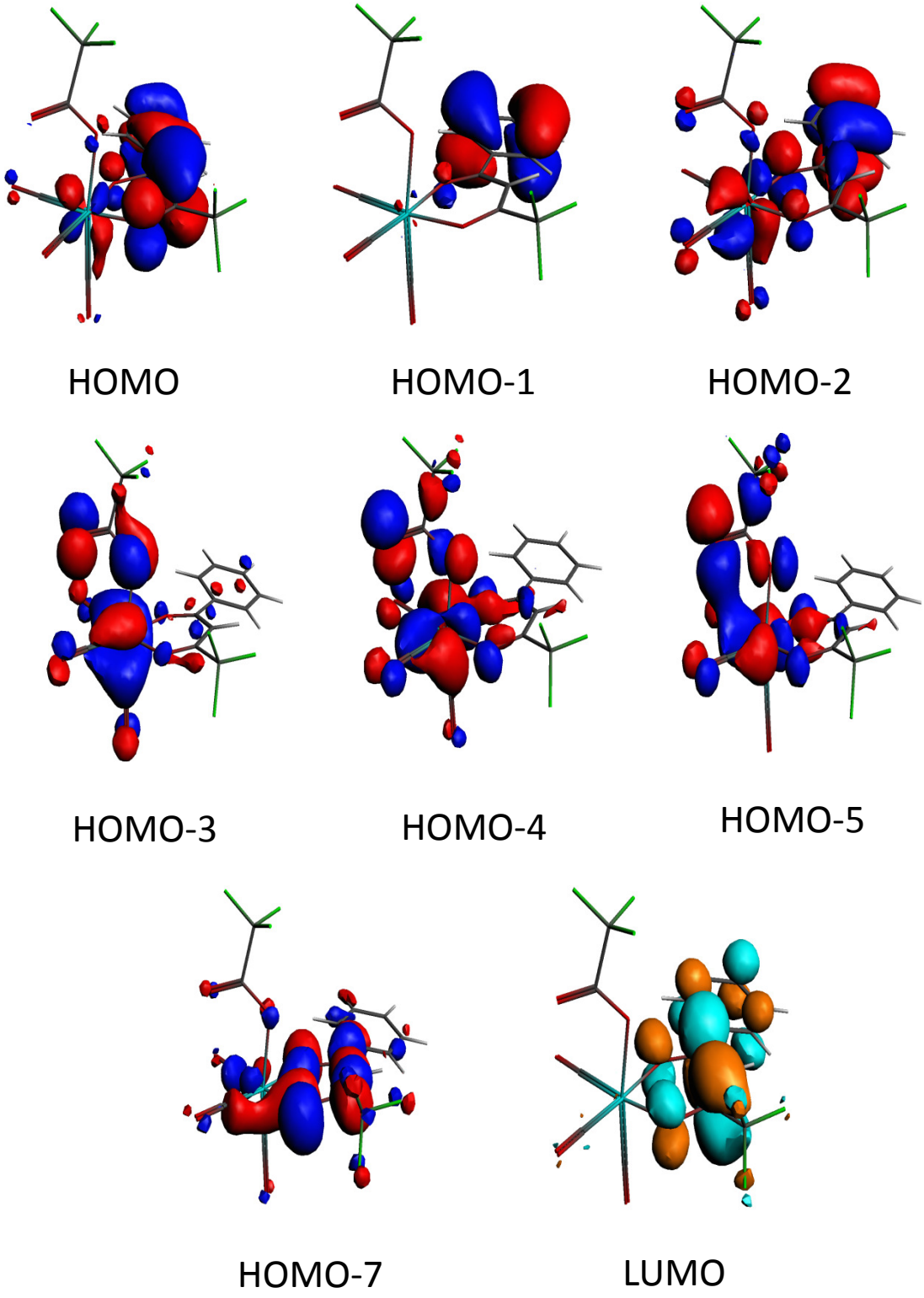

Figure S4. Spatial plots (isovalue = 0.03) of selected molecular orbitals for **Os-4** at ground-state optimized geometry.

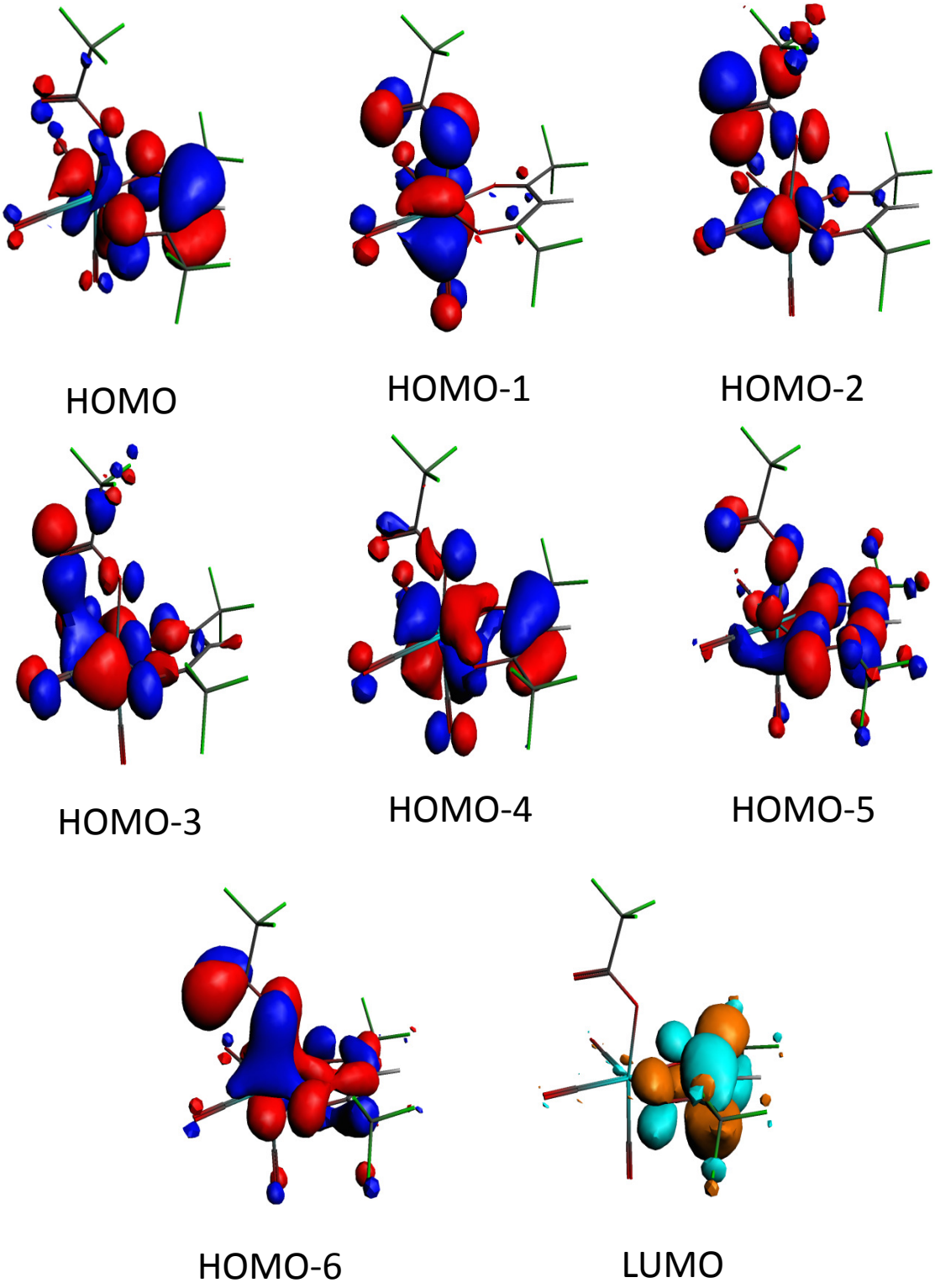

Figure S5. Spatial plots (isovalue = 0.03) of selected molecular orbitals for **Os-5** at ground-state optimized geometry.

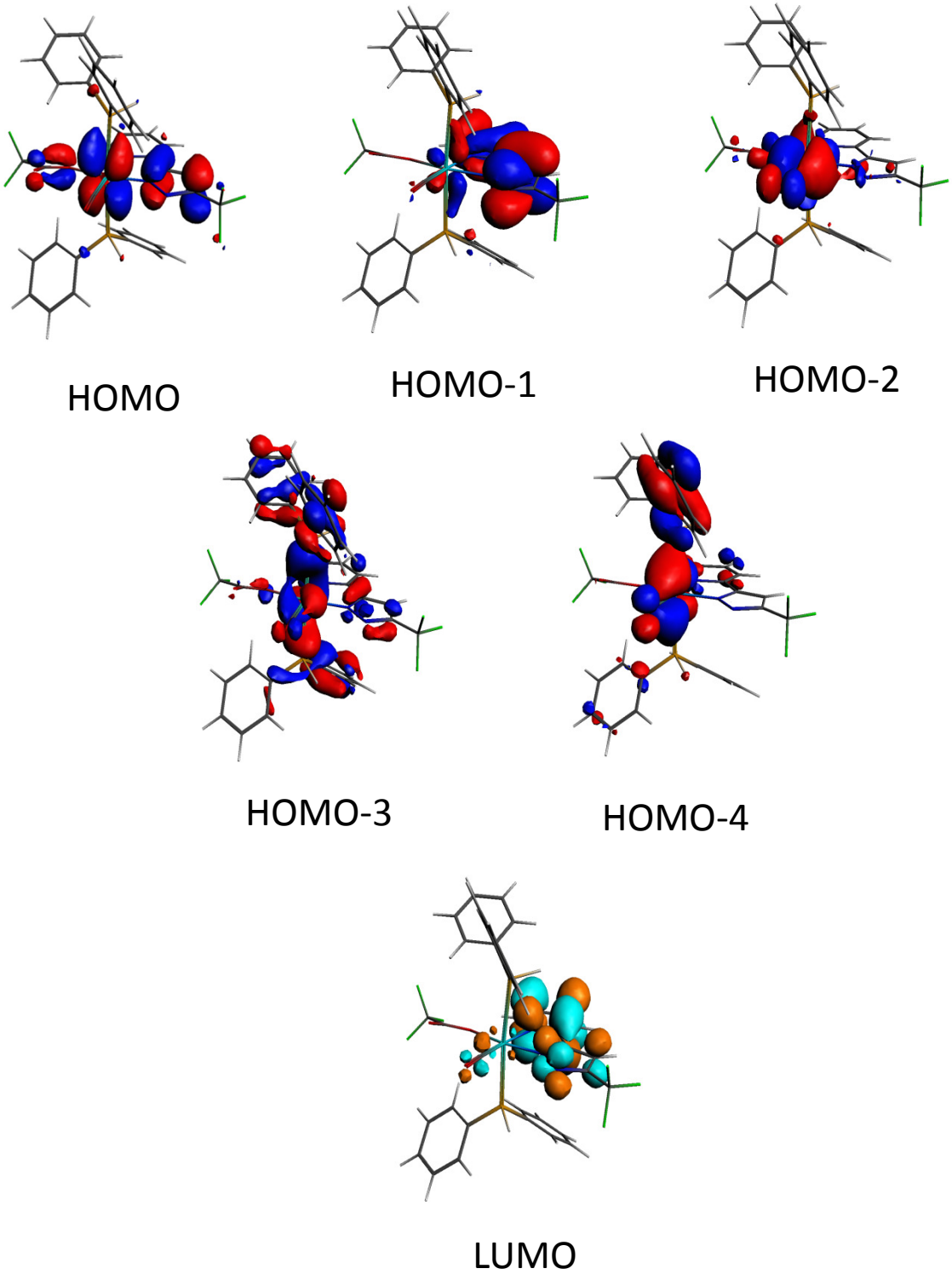

Figure S6 Spatial plots (isovalue = 0.03) of selected molecular orbitals for **Cu-1** at ground-state optimized geometry.

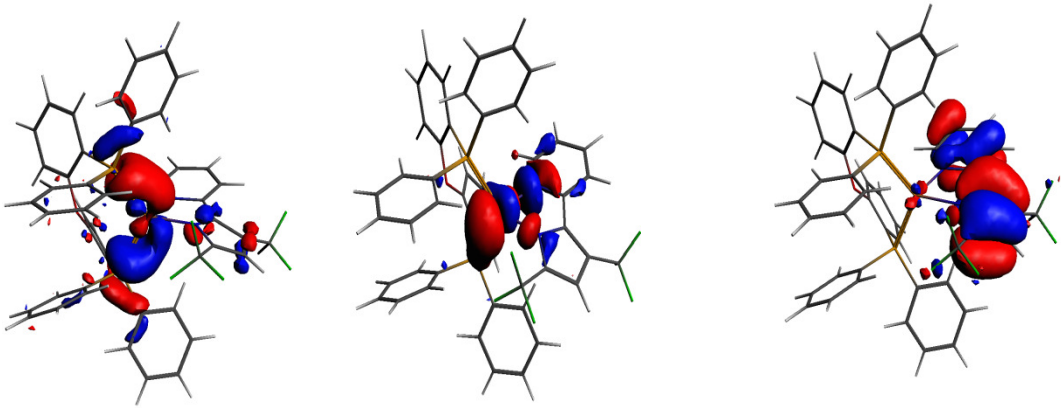

HOMO HOMO-1 HOMO-2

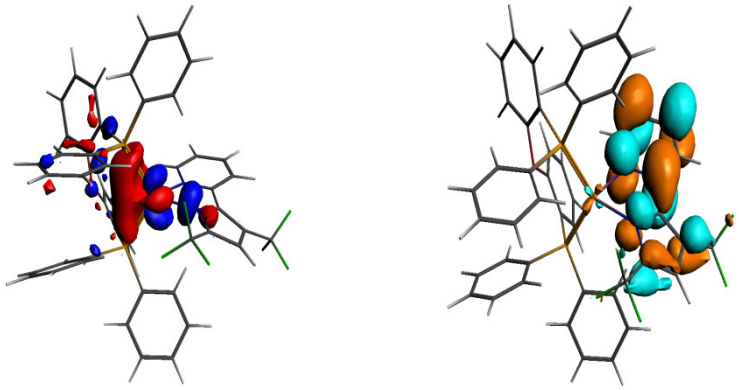

HOMO-3 LUMO

Figure S7. Spatial plots (isovalue = 0.03) of selected molecular orbitals for **Cu-2** at ground-state optimized geometry.

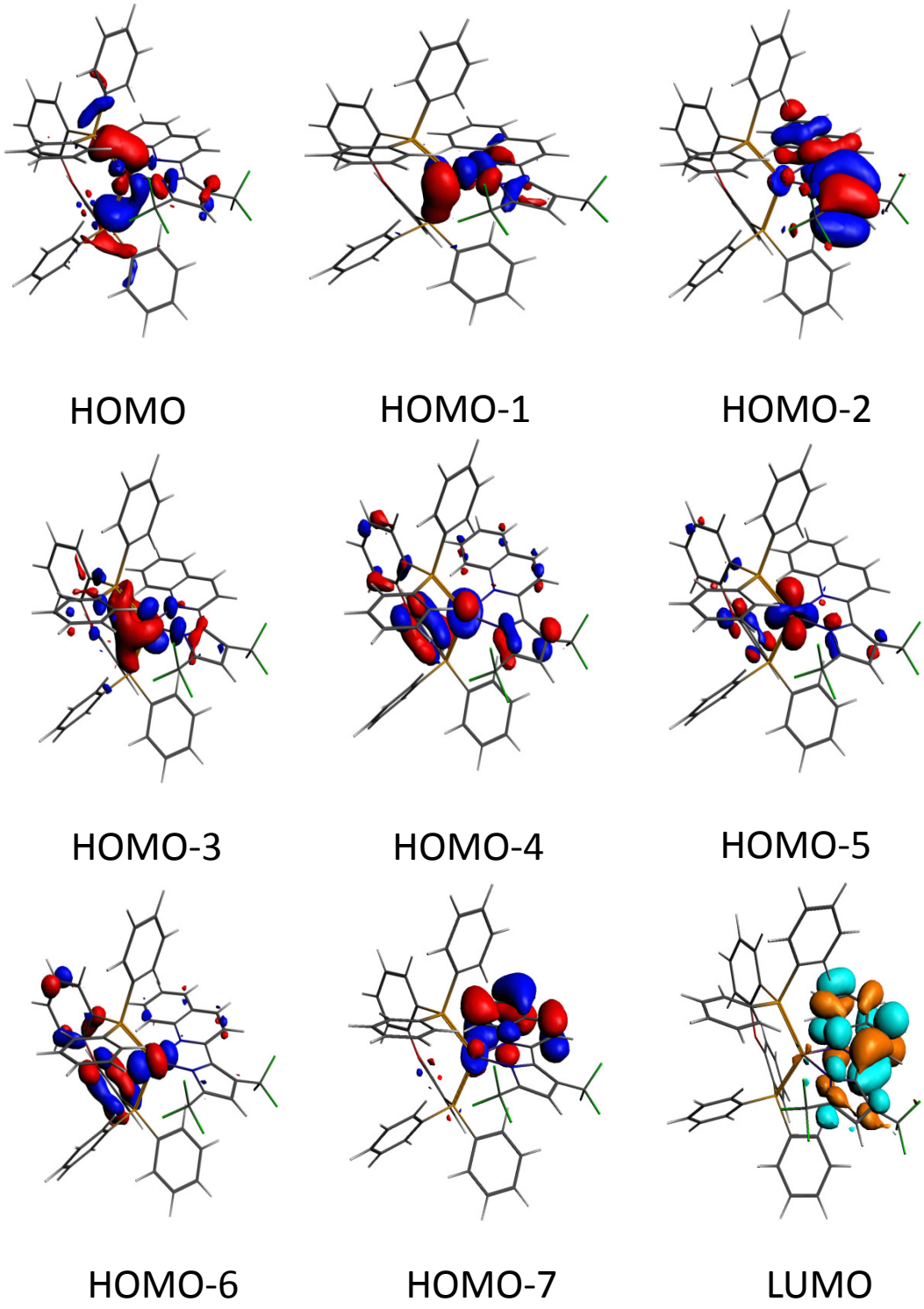

Figure S8. Spatial plots (isovalue = 0.03) of selected molecular orbitals for **Ag-1** at ground-state optimized geometry.

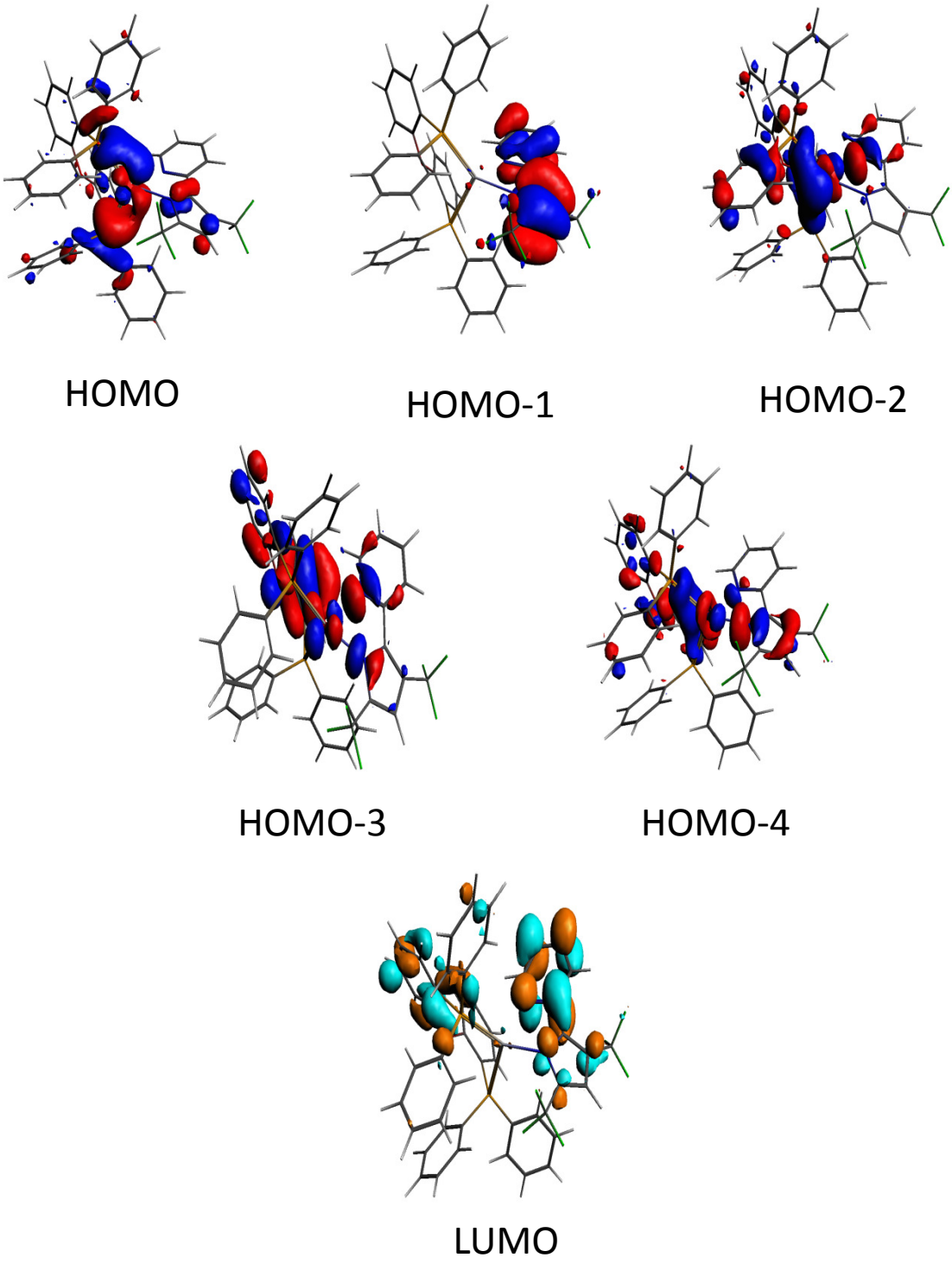

Figure S9. Spatial plots (isovalue = 0.03) of selected molecular orbitals for **Ag-2** at ground-state optimized geometry.

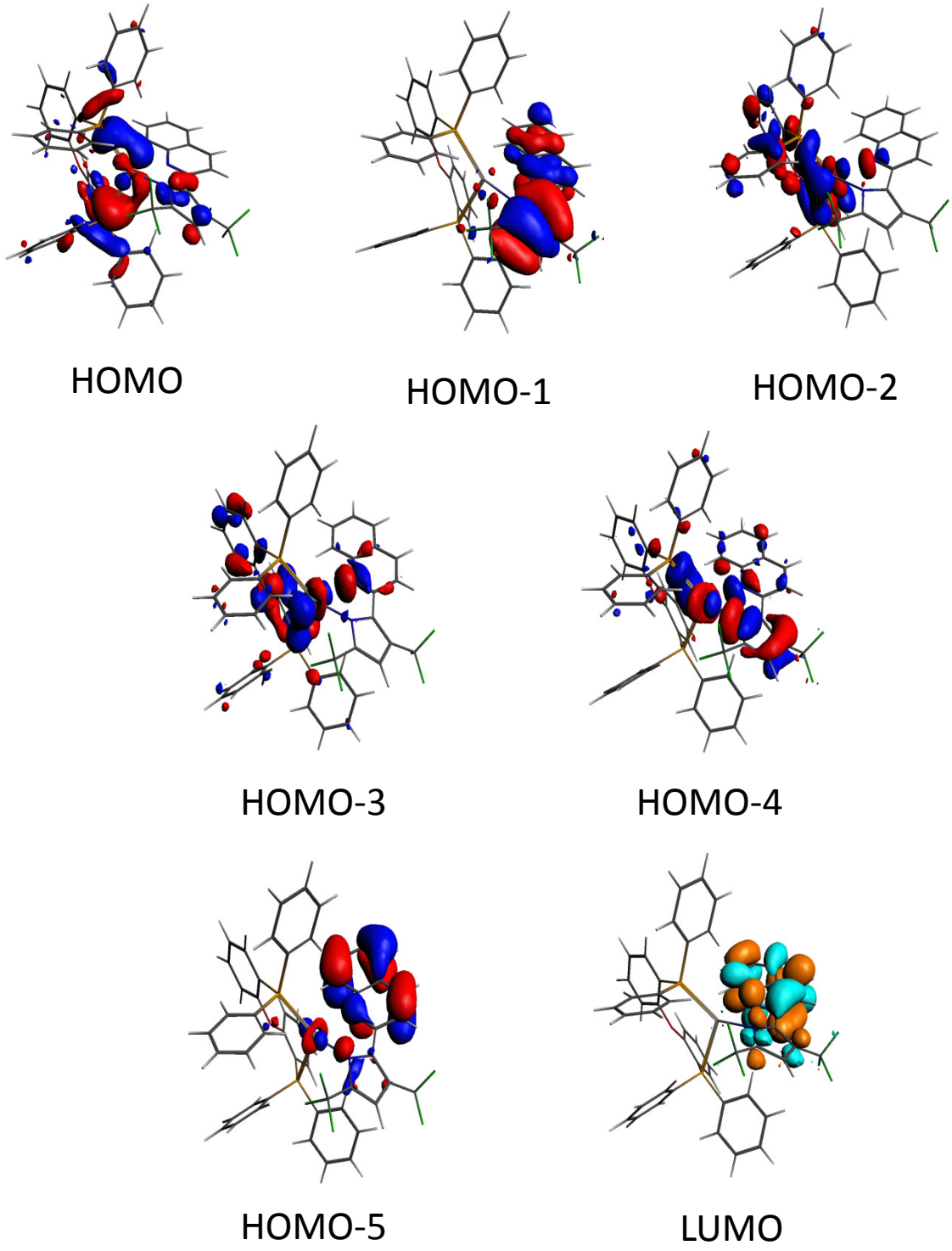

Figure S10. Spatial plots (isovalue = 0.03) of selected molecular orbitals for **Au-1** at ground-state optimized geometry.

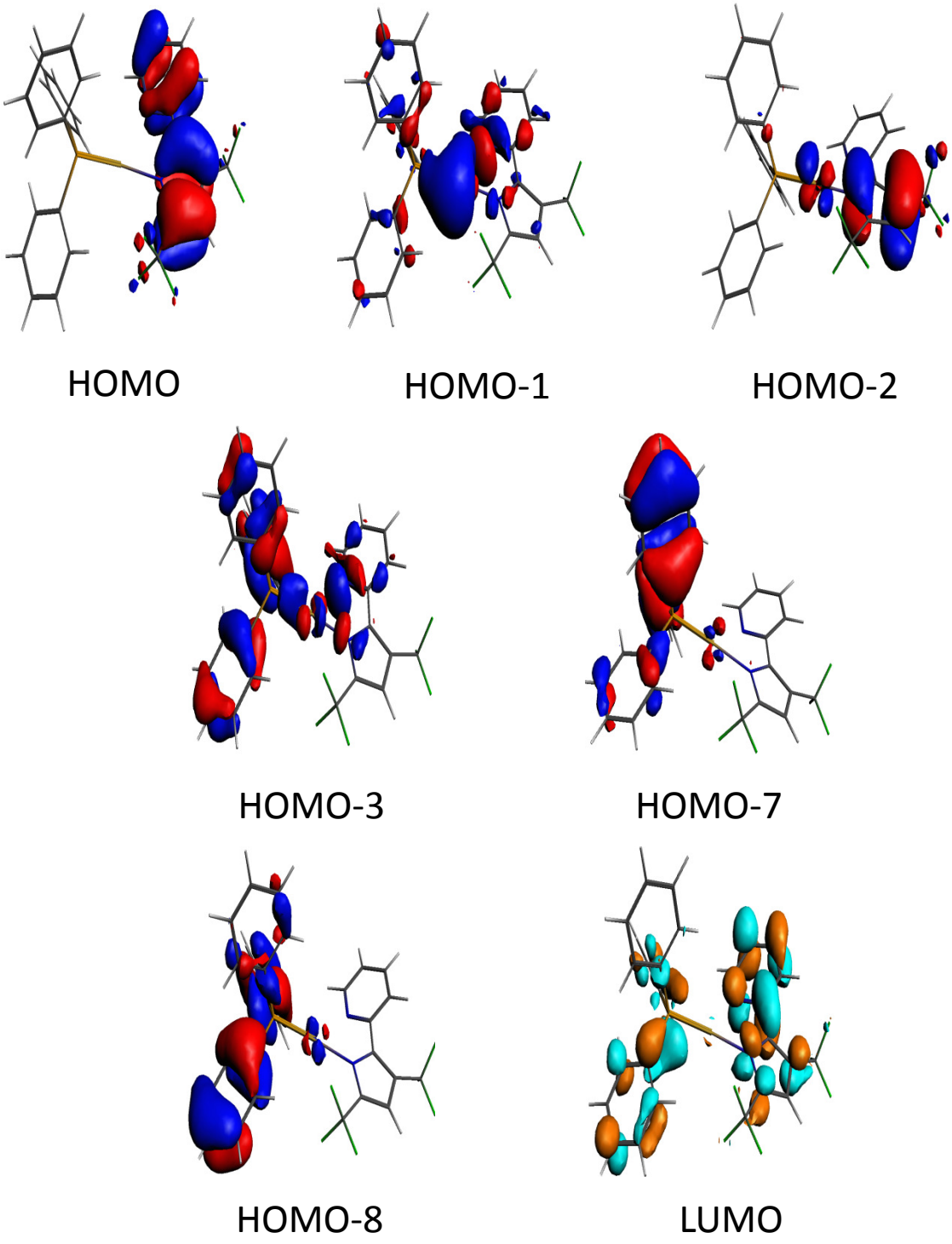

Figure S11. Spatial plots (isovalue = 0.03) of selected molecular orbitals for **Au-2** at ground-state optimized geometry.

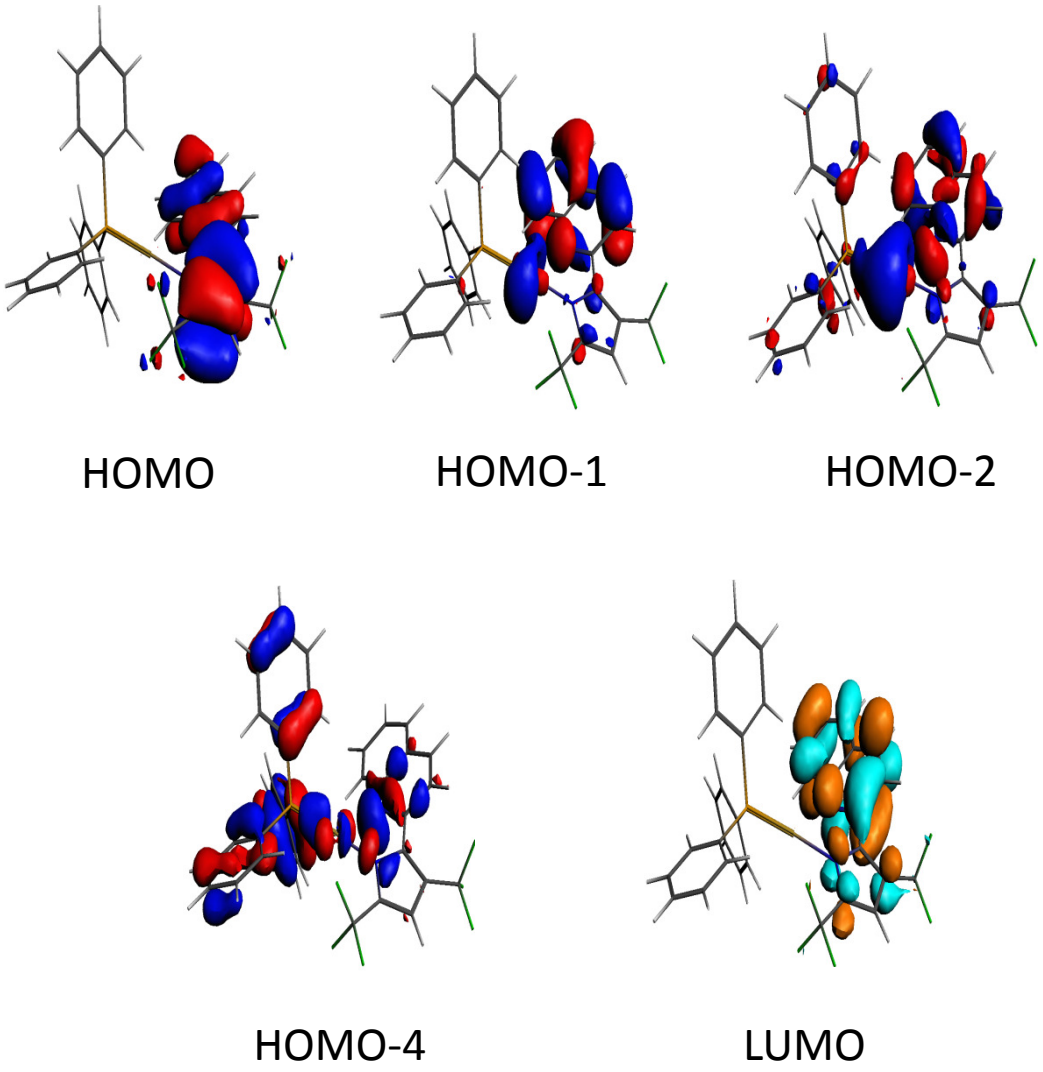

Figure S12. The SOC integrals (cm^{-1}) for **Os-7** between S_n (n=10) and T_m states (m=1-5).

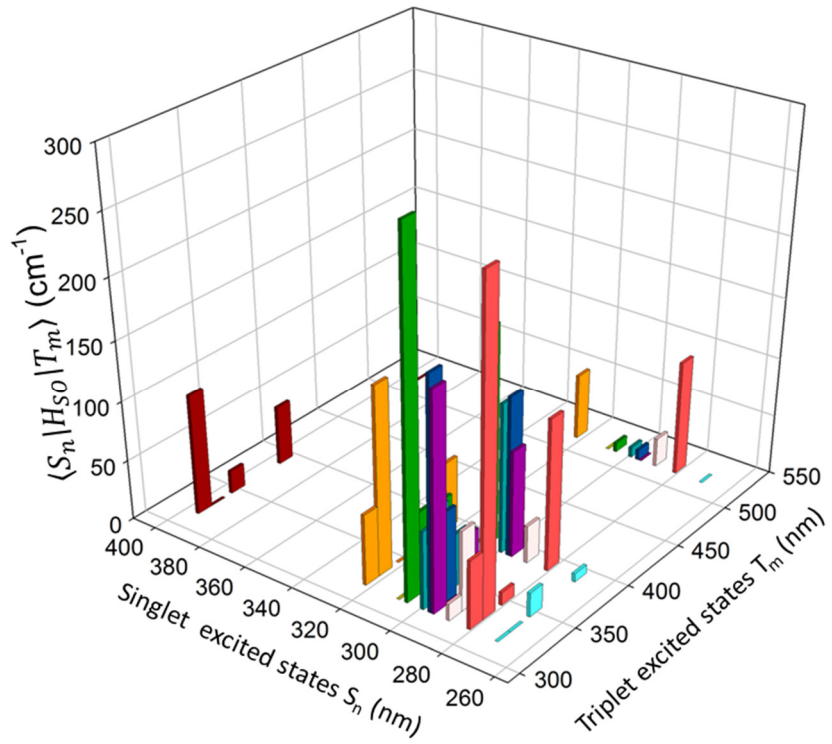

Figure S13. The SOC integrals (cm^{-1}) for **Os-8** between S_n (n=10) and T_m states (m=1-5).

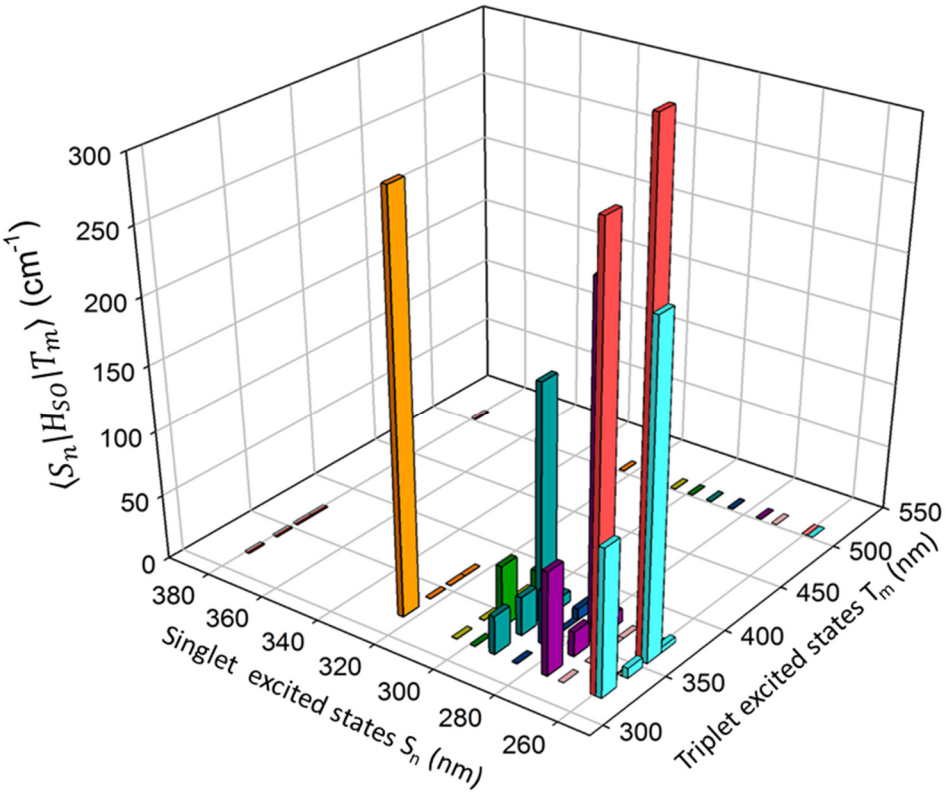

Figure S14. The SOC integrals (cm^{-1}) for **Os-9** between S_n (n=10) and T_m states (m=1-5).

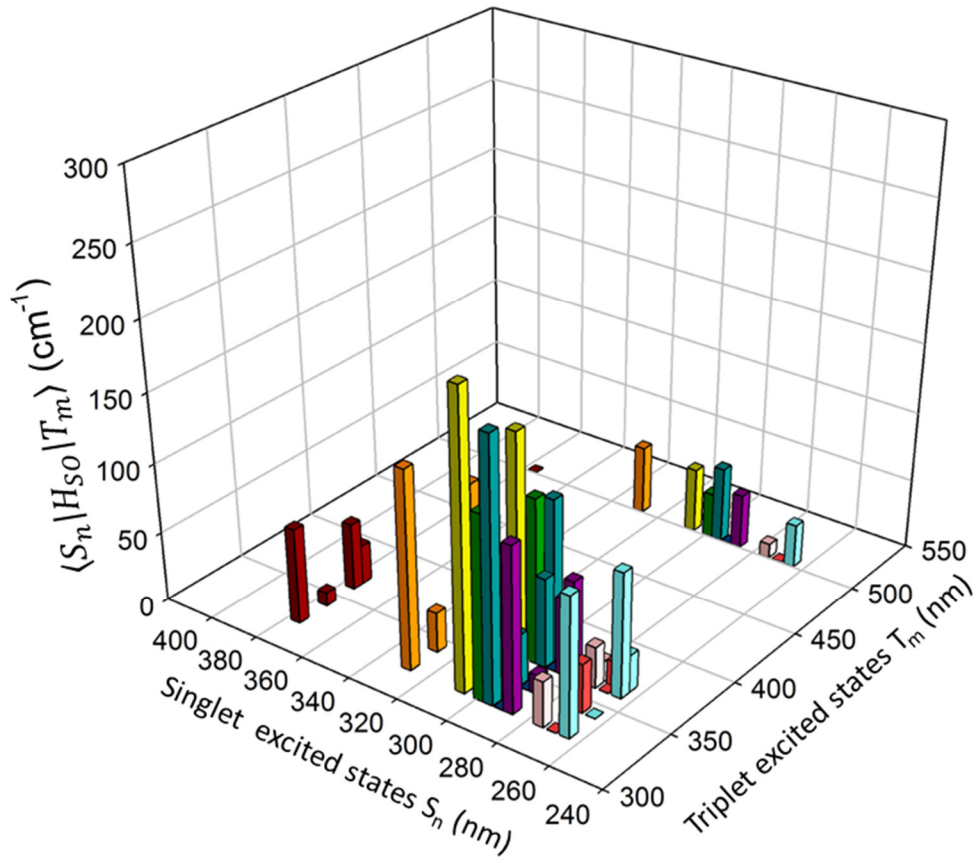

Complete reference for Gaussian09 (reference [8])

Gaussian 09, Revision C.01, Frisch, M. J.; Trucks, G. W.; Schlegel, H. B.; Scuseria, G. E.; Robb, M. A.; Cheeseman, J. R.; Scalmani, G.; Barone, V.; Mennucci, B.; Petersson, G. A.; Nakatsuji, H.; Caricato, M.; Li, X.; Hratchian, H. P.; Izmaylov, A. F.; Bloino, J.; Zheng, G.; Sonnenberg, J. L.; Hada, M.; Ehara, M.; Toyota, K.; Fukuda, R.; Hasegawa, J.; Ishida, M.; Nakajima, T.; Honda, Y.; Kitao, O.; Nakai, H.; Vreven, T.; Montgomery, Jr., J. A.; Peralta, J. E.; Ogliaro, F.; Bearpark, M.; Heyd, J. J.; Brothers, E.; Kudin, K. N.; Staroverov, V. N.; Kobayashi, R.; Normand, J.; Raghavachari, K.; Rendell, A.; Burant, J. C.; Iyengar, S. S.; Tomasi, J.; Cossi, M.; Rega, N.; Millam, J. M.; Klene, M.; Knox, J. E.; Cross, J. B.; Bakken, V.; Adamo, C.; Jaramillo, J.; Gomperts, R.; Stratmann, R. E.; Yazyev, O.; Austin, A. J.; Cammi, R.; Pomelli, C.; Ochterski, J. W.; Martin, R. L.; Morokuma, K.; Zakrzewski, V. G.; Voth, G. A.; Salvador, P.; Dannenberg, J. J.; Dapprich, S.; Daniels, A. D.; Farkas, Ö.; Foresman, J. B.; Ortiz, J. V.; Cioslowski, J.; Fox, D. J. Gaussian, Inc., Wallingford CT, 2010.